Asian Journal of Chemistry; Vol. 34, No. 10 (2022), 2664-2670

ASIAN JOURNAL OF CHEMISTRY

https://doi.org/10.14233/ajchem.2022.23955

Antibiofilm, Cytotoxicity and Release Studies of Green Synthesized ZnO Nanoparticles Embedded in Poly(Methyl Methacrylate) in Management of Cariogenic *Streptococcus mutans*

N. Ahalya, P. Dhamodhar*, N. Sanmati and Aditya Krishnakumar

Department of Biotechnology, M S Ramaiah Institute of Technology, Bangalore-560054, India

*Corresponding author: Fax: +91 80 23603124; Tel: +91 80 23603122; E-mail: dhamu.bio@gmail.com

Received: 7 June 2022; *Accepted*: 5 July 2022; *Published online*: 19 September 2022; AJC-20971

Nanoparticles exhibiting microbicidal and antibiofilm activity against *Streptococcus mutans* seems to be a promising prospect in the management of dental caries. In present study, zinc oxide nanoparticles were synthesized using *Rosa bracteata* extract and characterized using UV visible spectroscopy, SEM and XRD. The synthesized ZnO nanoparticles exhibited a strong absorbance at 390 nm, with an average crystalline size of 118 nm. The SEM analysis showed nanowire like structures with a size ranging between 65-150 nm. The ZnO nanoparticles exhibited antibacterial activity against *Streptococcus mutans* at a concentration of 100 µg/mL. There was a significant reduction in the number of *S. mutans* forming biofilm, in the presence 100 µg/mL of ZnO nanoparticles. Further, ZnO nanoparticles were embedded in the dental prosthetic material poly(methyl methacrylate) to form PMMA-ZnO nanocomposites and the amount of ZnO nanoparticles released from the nanocomposite was measured. Further, the ZnO nanoparticles at 100 µg/mL concentration were found to be non-toxic on the HaCaT cell lines. This study proves that the green synthesized ZnO nanoparticles incorporated into the dental prosthetics can be used in the control and prevention of secondary dental caries.

Keywords: Dental caries, Poly(methyl methacrylate), ZnO nanocomposites, Antibiofilm, *Streptococcus mutans*, Cytotoxicity.

INTRODUCTION

In dental caries, the demineralization of the tooth enamel occurs and subsequently results in deep cavities due to the presence of cariogenic bacteria like *Streptococcus mutans*, *Lactobacillus* spp., *etc*. [1]. *S. mutans*, a Gram-positive, facultative anaerobe which forms biofilm. Biofilms are a community of bacterial cells that are surrounded by exopolysaccharide layer and hence adhere to the substratum like tooth surfaces, bone, glass, metals, *etc*. [2]. Biofilm formation is driven by many virulence factors like glucosyltransferases, glucan binding proteins, exopolysaccharide formation, salivary proteins, *etc*. Factors like diet, genetic inheritance and poor oral hygiene also aid in the biofilm formation [3,4]. The stream of biochemical pathways resulting in its acidogenicity and aciduricity contribute to the tenacity of biofilm formation and henceforth, the infection [5]. This results in the persistence and reoccurrence of dental caries.

The conventional treatment of dental caries employs the use of antibiotics, fluoride application, dental filling, dental crown, *etc*. Most of these treat the symptoms but not the cause, except antibiotics and fluorides. One of the main drawbacks of antibiotics is the extermination of healthy microflora and increasing bacterial antibiotic resistance. This in turn contributes to the reoccurrence of dental caries. The disadvantage of fluoride applications is that it causes dental fluorosis on repeated usage. Hence, various approaches to eliminate the biofilms of *S. mutans* have been studied ranging from the use of products from other microbes, plants, antibodies, macrolides, block-*co*-polymers, *etc*. [6]. In addition to this, nanoparticles like silver, calcium fluoride and ZnO have shown significant antimicrobial, antibiofilm activity and therefore can be used as a novel approach to eliminate the biofilm [7,8].

ZnO nanoparticles are widely known for their antibacterial properties and finds wide range of applications in biomedical field [9,10]. These are known for their bactericidal characteristics by the generation of reactive oxygen species (ROS) like $^{\bullet}H_2O_2$ (hydrogen peroxide), OH^- (hydroxide), *etc*. ZnO nanoparticles are used greatly in medical devices, cosmetic, pharmaceutical and food industries [11,12]. Chemical synthesis of

ZnO nanoparticles has an advantage of size and geometrical variation. However, the reagents involved in chemical synthesis are found to be toxic [13]. Green methods for synthesizing nanoparticles are safe and eco-friendly and therefore a better alternative to the chemical methods. Green synthesis of ZnO nanoparticles using plant extracts as reducing agents results in a good size reduction usually in the range of 100-200 nm [14,15].

Poly(methyl methacrylate) (PMMA) is a material that has been used widely in dental prosthetics over decades. The mechanical property of PMMA and its effects on the oral cells and tissues are thoroughly understood [15,16]. However, PMMA does not exhibit antibacterial activity. One way of incorporating antibacterial activity in PMMA, is by infusing the nanoparticles into it. The PMMA-ZnO nanocomposite materials as a promising material for denture bases are becoming increasingly popular among scientists and dentists [17,18]. A thin layer of saliva is present between the denture base and oral mucosa. Because of this, the nanoparticles that are released from the dental prosthetic material can penetrate the underlying tissue and exert an antibacterial action [19,20].

In present study, ZnO nanoparticles were green synthesized using *Rosa bracteate* and characterized. The nanoparticles were tested for its antibacterial and antibiofilm activity against *S. mutans*. Further, the nanoparticles were incorporated into PMMA to form PMMA-ZnO nanocomposites and their release rate was studied. The cytotoxicity of the nanoparticles was also evaluated.

EXPERIMENTAL

Synthesis of ZnO nanoparticles: Dried and powdered petals of *Rosa bracteate* was used as a reducing agent for the synthesis of ZnO nanoparticles. About 5 g of *R. bracteate* powder was added to 100 mL of water and boiled for 1 h. This extract (50 mL) was added to 200 mL of zinc acetate (0.2 M) and stirred at around 30 ºC for about 1 h. Sodium hydroxide solution (3 M) was added gradually until an alkaline pH was reached. The obtained ZnO precipitate was centrifuged at 10000 rpm for 10 min. The pellet was washed with water three times and dried overnight at 60 ºC and then placed in a muffle furnace for 1 h at 400 ºC. The synthesized ZnO nanoparticles was subjected to X-ray diffraction (XRD), scanning electron microscopy (SEM) and UV-Vis spectroscopy for characterization [21,22].

Antibacterial activity of ZnO nanoparticles: The ZnO nanoparticles were tested for its antibacterial activity against *S. mutans* by agar well diffusion method. The *S. mutans* (MTCC 497) received from Institute of Microbial Technology, Chandigarh, India was then inoculated onto the sterile Muller Hinton Agar (MHA) plates. The wells were punctured on the surface of the plates and various concentrations of ZnO nanoparticles (100-500 µg/mL) were added. Streptomycin (25 µg) was used as a control. The plates were then incubated for 24-48 h at 37 ºC. After the incubation period, the antibacterial activity was determined by measuring the zone of inhibition [23].

Antibiofilm activity of ZnO nanoparticles: The antibiofilm activity of ZnO nanoparticles on *S. mutans* biofilm formation was carried out as described by O'Toole [24]. The biofilm formation was evaluated by the crystal violet assay. The overnight culture of *S. mutans* (MTCC 497) was diluted to 1:100 with Todd Hewitt Broth and a concentration of 100 µg/mL of the synthesized ZnO nanoparticles was added. This inoculum (100 µL) was added to each well of the microtiter plate. The wells were then incubated at different intervals of time at 37 ºC. The wells were subsequently washed to remove the excess cells. To each well, 125 µL of crystal violet stain was added and incubated for 20 min. The excess stain was washed off gently and the plates were dried overnight. The adhered crystal violet was solubilized by adding 125 µL of 30% acetic acid and incubated for 15-20 min. The absorbance was measured at 550 nm using 30% acetic acid as blank. The number of cells contributing to the biofilm formation was then correlated to the McFarland scale. The same procedure was followed for establishing the biofilm formation in control, wherein ZnO was not added and the cell density was determined. The absorbance values obtained from the control and test samples were used to calculate the percentage antibiofilm activity [25].

$$\text{Antibiofilm activity (\%)} = \frac{\text{Control OD} - \text{Test OD}}{\text{Control OD}} \times 100$$

Preparation of PMMA-ZnO nanocomposites: The PMMA-ZnO nanocomposite was prepared as described by Cierech *et al.* [26]. The PMMA polymer powder was mixed with liquid monomer in the volume ratio of 3:1. The ZnO nanopowder was suspended in a liquid monomer of PMMA resin such that 5% (w/v) of ZnO nanoparticles concentration was achieved. The mixture was shaken in a shaker and sonicated. The dough was then made into tiny balls, which were further utilized for release studies of ZnO nanoparticles [26].

Release rate of ZnO nanoparticles from poly(methyl methacrylate) (PMMA): The nanocomposite ZnO-PMMA balls with a concentration of 5% ZnO was added into ten beakers. Artificial saliva was prepared as described elsewhere [27]. To these beakers, artificial saliva and phosphate buffer was added in the ratio of 1:1 and the final volume was amounted to 5 mL. This was done so as to mimic the conditions in the oral cavity. The beakers were then kept in an incubator at 37 ºC. The optical density of ZnO nanoparticles was measured at various time intervals at 390 nm, which corresponds to the amount of ZnO nanoparticles released [28]. The amount of ZnO nanoparticles released from PMMA-ZnO nanocomposite was further estimated and their release rate was measured at various pH.

Cytotoxicity evaluation of ZnO nanoparticles: The cytotoxicity of ZnO nanoparticles was evaluated on HaCaT cell lines. About 200 µL of the cell suspension was added to each well and kept still to enable the cells to cling onto the well. To these wells, ZnO nanoparticle concentrations ranging from 10 µg to 1000 µg was added. Camptothecin was used as a reference compound. The wells were then incubated for 12 h at 37 ºC and 5% CO_2. The MTT agent was added to a volume of 10% of the total volume in each well. The 96-well plate was further covered in aluminium foil to prevent any light exposure. The plate was then incubated at 37 ºC and 5% CO_2

for 3 h. DMSO was added to each well in equal volume as that of cell culture and the plate was kept on a gyratory shaker to encourage better diminution. The absorbance at 570 nm was measured and the viability was estimated. The MTT assay was carried out at Stellixir Biotech Pvt. Ltd., Bangalore, India.

RESULTS AND DISCUSSION

UV-visible studies: ZnO nanoparticles were subjected to a wavelength scan in the UV-vis range of the electromagnetic spectrum. Fig. 1 represents the UV-visible spectra of the synthesized ZnO nanoparticles using *Rosa bracteata*. The maximum absorbance was observed at 390 nm, which is similar to the previous results [22,29,30]. The absorbance at 390 nm confirmed the change of initial material zinc acetate to ZnO nanoparticle [31,32]. Further, there were no peaks after the ZnO peak suggesting that dopants are not present in the sample. Thus, the UV-vis analysis confirms the presence of ZnO nanoparticles as the maximum absorbance falls under the range of 315-400 nm, which is a characteristic property of ZnO nanoparticles [33-35].

SEM studies: The green synthesized ZnO nanoparticles using *R. bracteata* were analyzed for their size and morphology

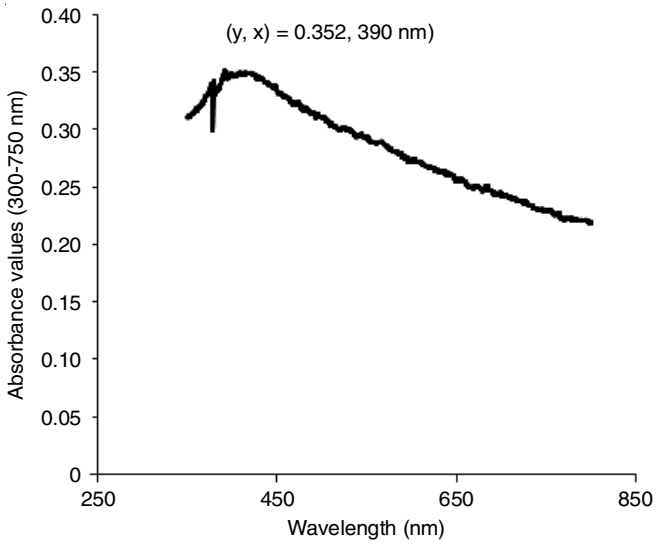

Fig. 1. UV-visible spectra of the green synthesized ZnO NPs

by SEM. The polyhedral, nanoflowers and nanowire like structures were observed and the nanoparticle size range was between 65 to 150 nm (Fig. 2). This size range obtained is in agreement with the size of ZnO nanoparticles reported in literature [36].

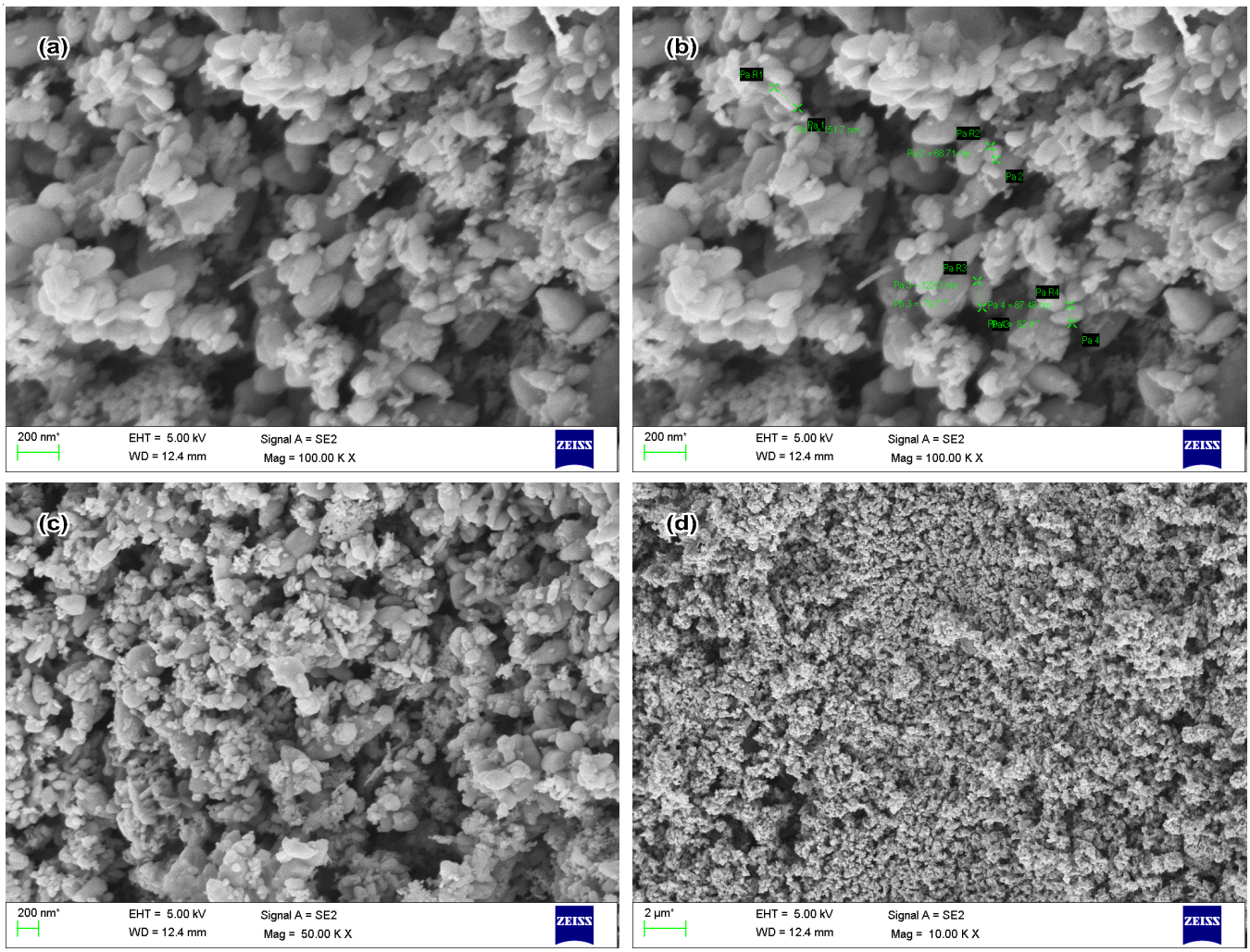

Fig. 2. SEM images of the green synthesized ZnO nanoparticles

XRD studies: The X-ray diffraction of ZnO nanoparticles showed intense Bragg's reflection with 2θ values of 31.2251º, 33.8859º, 35.7043º, 47.1353º, 56.1950º, 62.4982º, 67.5449º and 68.7201º (Fig. 3). The corresponding miller indices were (100), (002), (101), (102), (110), (103), (112) and (201), which was similar to the results obtained by Rekha *et al.* [37] and the peaks were similar to the JCPDS standard (JCPDS: 36-1451). As there were no additional 2θ peaks, this proves that impurities were absent. Using Scherrer's relation *i.e.* $D = K\lambda/(\beta \cos \theta)$ the crystalline size for each θ value was calculated. The average crystalline size was found to be 118 nm.

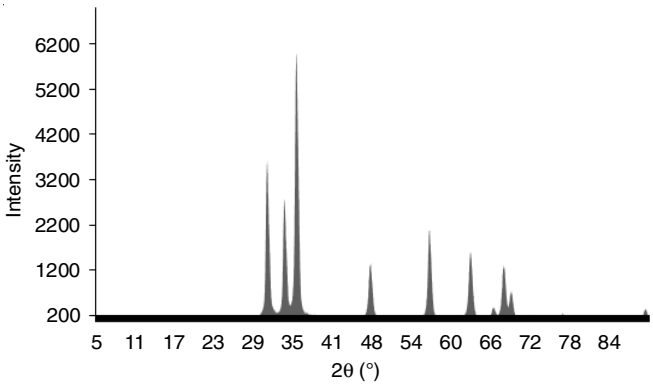

Fig. 3. XRD spectrum of the green synthesized ZnO NPs

Antibacterial activity: It was observed that the standard antibiotic streptomycin had the highest zone of inhibition against *S. mutans* (Table-1). The zone of inhibition around the wells loaded with ZnO nanoparticles was observed, which confirms that the green synthesized ZnO nanoparticles exhibit antibacterial activity. Amongst the varying ZnO nanoparticle concentrations, the highest zone of inhibition observed was for the concentration 500 µg/mL.

TABLE-1
AVERAGE ZONE OF INHIBITION OF DIFFERENT CONCENTRATION OF ZnO NANOPARTICLES AGAINST *S. mutans*

Concentration of ZnO NPs (µg/mL)	Average zone of inhibition (mm)
100	10.25 ± 1.70
200	11.25 ± 1.25
300	13.75 ± 1.25
400	18.50 ± 3.10
500	23.25 ± 2.21
Streptomycin	25.66 ± 2.51

Zinc oxide nanoparticles has proved to be effective antimicrobial agent for pathogenic bacteria like *P. aeruginosa, P. alcaligenes, E. coli, S. pyogenes, S. aureus, S. typhimurium, P. mirabilis, E. faecalis* and *E. aerogenes* [38-40]. Zinc oxide nanoparticles prove to be effective antimicrobial agents as they increase the bacterial membrane permeability leading to the disturbance in the bacterial membrane proteins [41].

Antibiofilm activity of ZnO nanoparticles: The biofilm formation by *S. mutans* was quantified by microtiter method and the growth was determined based on the absorbance at 550 nm for 0-5 h with an interval of 1 h between readings. The obtained absorbance values were related to the McFarland's standard plot and the number of cells forming the biofilm was determined. Initially in the control sample, at 0th h, biofilm formation commenced with 0.191×10^8 CFU/mL, a dip at 2nd h was observed, indicating the lag phase of the growth of *S. mutans* followed by which it reached 0.369×10^8 CFU/mL at 5th h of incubation (Fig. 4). Similar trend in the biofilm formation was reported by Kulshrestha *et al.* [42].

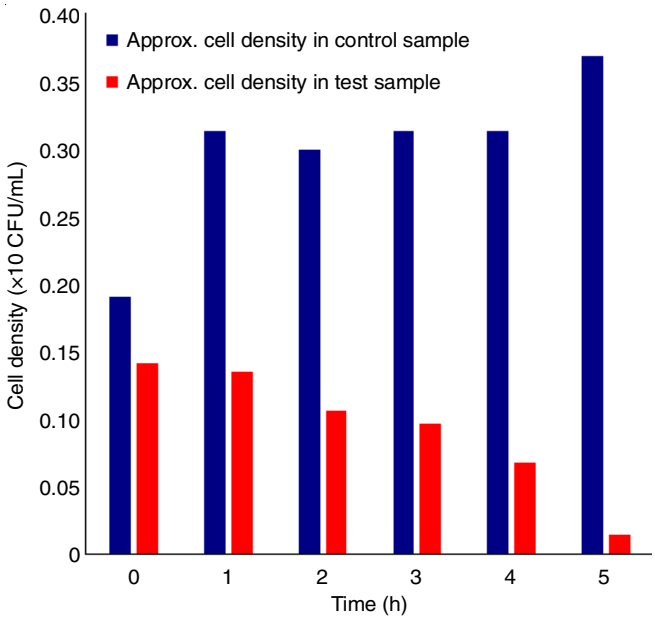

Fig. 4. Antibiofilm assay of ZnO nanoparticles

Subsequently, the antibiofilm activity of green synthesized ZnO nanoparticles was studied with the addition of 100 µg/mL of ZnO nanoparticles. A 0.142×10^8 CFU/mL was present at the 0th h. There was a constant decrease in the cell density throughout the 5 h and at the 5th h the approximate cell density in the test sample was found to be 0.015×10^8 CFU/mL (Fig. 4). The number of bacteria forming biofilm had significantly decreased in the presence of ZnO nanoparticles when compared with the control samples.

It was observed that as the time of incubation increased, the number of cells forming the biofilm decreased. At the 5th h of incubation, the antibiofilm activity was around 95%. Similar results were reported in a study by Vijayakumar & Vaseeharan [43] where maximum biofilm inhibition was seen at 75 µg/mL when incubated for 24 h. In the present study, when 100 µg/mL of ZnO nanoparticles was used, the biofilm formation of *S. mutans* was maximum inhibited in the 5th h of incubation. Zinc oxide nanoparticles have also been reported to prevent biofilm formation of *P. aeuroginosa* at a concentration of 64 µg/mL at 2 h incubation [44]. Silver nanoparticles coated on catheters have shown to inhibit the formation of biofilms by *S. aureus* [45]. An anti-biofilm effect of ZnO nanoparticles at a concentration of 50 to 350 µg/mL reduced pre-formed biofilm of *P. aeruginosa* [46]. Zinc oxide nanoparticles of smaller size *i.e.*, less than 20 nm has better anti-biofilm activity may be due to the higher penetration through the bacterial cell wall than the larger nanoparticles [47].

Release rate studies: The release of ZnO nanoparticles from the PMMA-ZnO nanocomposite into the artificial saliva was studied. Artificial saliva was used as a buffer system to recreate the natural salivary environment *in vitro*. The release rate was investigated at a salivary pH ranging from 6.5-7.5 with an increment of 0.1 at 37 ºC. The release of ZnO nanoparticles was determined at different time intervals and pH. Overall, the highest release rate over time was observed at the pH of 7.1 and the lowest at pH 6.7 (Fig. 5). The release of ZnO nanoparticles from the PMMA-ZnO composite confirms its potential in the management of secondary caries as it can have an antimicrobial effect and inhibit biofilm formation of cariogenic bacteria. However, the amount of ZnO nanoparticles released needs to be optimized prior to its use in caries control.

Cytotoxicity evaluation: The MTT assay was performed to study the toxicity of ZnO nanoparticles on HaCaT cell lines (Fig. 6). The cytotoxicity of the ZnO nanoparticles was evaluated (Fig. 7) and Fig. 8 shows the cell viability percentage at various concentrations of ZnO nanoparticles. At a concentration of 100 µg/mL, the ZnO nanoparticles was found to be non-toxic on the cell lines tested. A sharp reduction in the absorbance value was observed beyond 250 µg/mL of ZnO. This reveals that the ZnO nanoparticles had a toxic effect on the cells from 250 µg/mL, which was similar to the results obtained by Nemati *et al.* [48]. As the antibiofilm activity and antimicrobial activity of ZnO nanoparticles on *S. mutans* were also observed at 100 µg/mL, it can be concluded that a concentration of 100 µg/mL in dental prosthetics would prove to be sufficient to prevent secondary dental caries. The results obtained in this study were in concurrence with that of Kulshrestha *et al.* [42]. Moreover, in earlier studies, it was established that green synthesized zinc oxide nanoparticles from *S. muticum* had median lethal concentration (IC_{50}) value of 150 µg/mL at 48 h exposure [49], while the ZnO nanoparticles synthesized from *Andrographis paniculata* showed anticancer activity at 250 µg/mL against He La and Hep-2 cell lines [50].

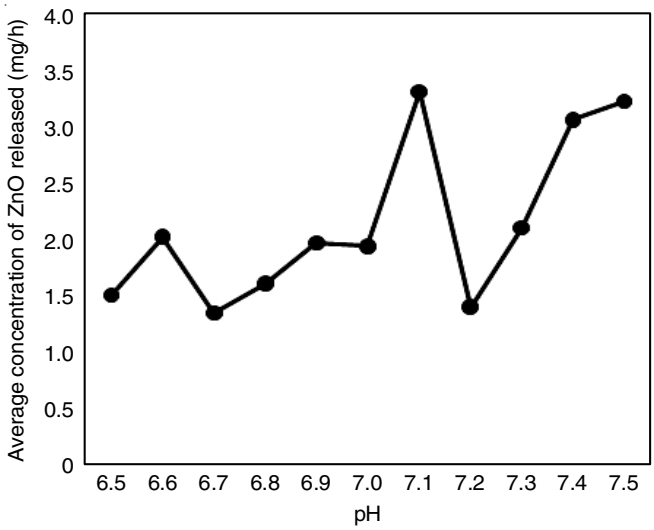

Fig. 5. Release rate studies of ZnO from PMMA-ZnO nanocomposite

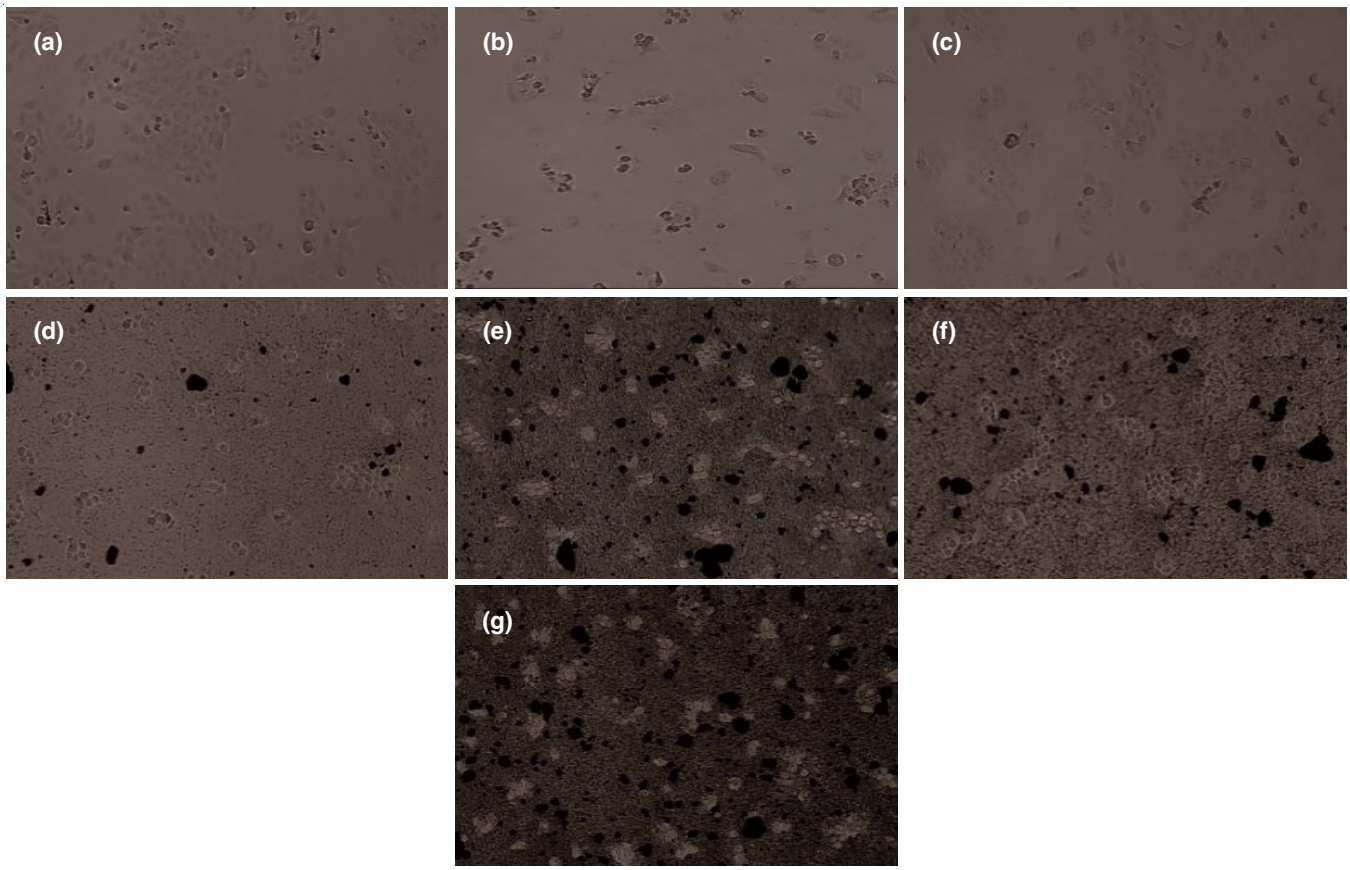

Fig. 6. Cytotoxicity evaluation of ZnO nanoparticles on Ha Cat cell lines (a: untreated sample, b: treated with 0.5 µM camptothecin, c-g: treated with 100, 250, 500, 750 and 1000 µg/mL ZnO NPs respectively)

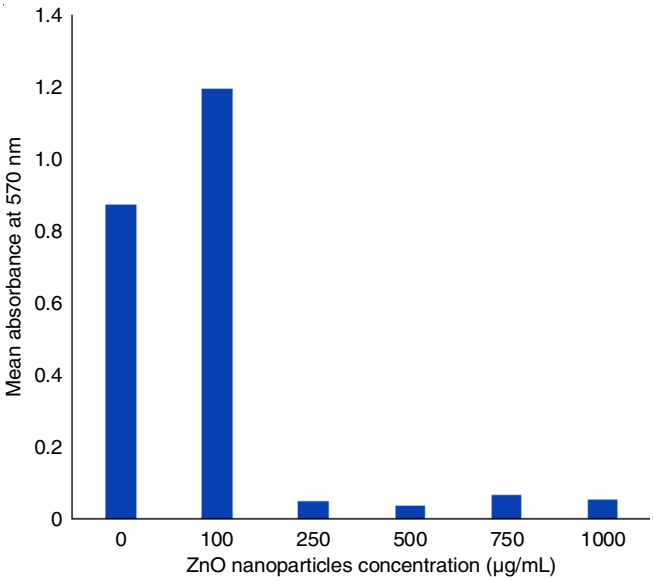

Fig. 7. ZnO cytotoxicity evaluation

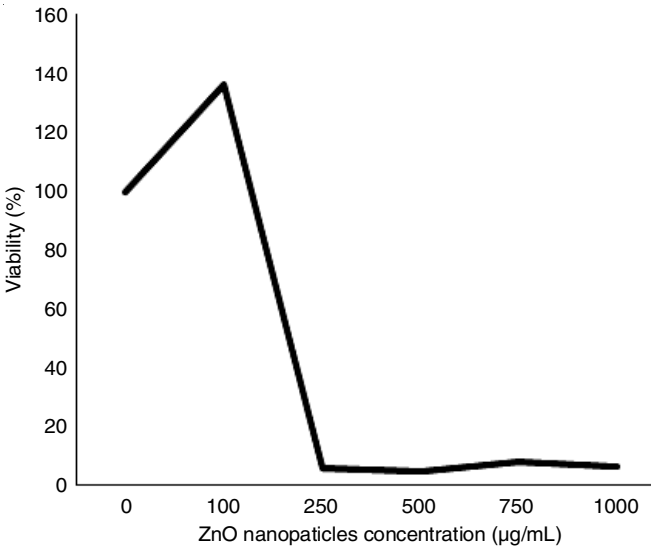

Fig. 8. Cell viability % at various concentrations of ZnO NPs

Conclusion

In present study, zinc oxide nanoparticles synthesized using *Rosa bracteate* was tested for their antimicrobial activity and antibiofilm activity. The results showed that synthesized nanoparticles were effective against *Streptococcus mutans* in preventing the formation of biofilm and exhibited antimicrobial property. Characterization studies revealed the crystalline ZnO nanoparticles having an average size of 118 nm. The ZnO nanoparticles were incorporated into dental prosthetic material (PMMA) and evaluated for their cytotoxicity and release studies. From the results, it can be concluded that the PMMA-ZnO composites can be used in the control and management of dental caries.

CONFLICT OF INTEREST

The authors declare that there is no conflict of interests regarding the publication of this article.

REFERENCES

1. V.P. Mathur and J.K. Dhillon, *Int. J. Pediatr.*, **85**, 202 (2018).
2. X. Chen, E.B.M. Daliri, N. Kim, J.R. Kim, D. Yoo and D.H. Oh, *Pathogens*, **9**, 569 (2020); https://doi.org/10.3390/pathogens9070569
3. A.P.V. Colombo and A.C.R. Tanner, *J. Dent. Res.*, **98**, 373 (2019); https://doi.org/10.1177/0022034519830686
4. K. Jhajharia, L.K. Mehta, A. Parolia and K.V. Shetty, *J. Int. Soc. Prev. Community Dent.*, **5**, 1 (2015); https://doi.org/10.4103/2231-0762.151956
5. N.J. Lin, *Dent. Mater.*, **33**, 667 (2017); https://doi.org/10.1016/j.dental.2017.03.003
6. A.M. Scharnow, A.E. Solinski and W.M. Wuest, *MedChemComm*, **10**, 1057 (2019); https://doi.org/10.1039/C9MD00015A
7. M.M. Al-Ansari, N.D. Al-Dahmash and A.J.A. Ranjitsingh, *J. Infect. Public Health*, **14**, 324 (2021); https://doi.org/10.1016/j.jiph.2020.12.016
8. M. Lukomska-Szymanska, B. Zarzycka, J. Grzegorczyk, K. Sokolowski, K. Poltorak, J. Sokolowski and B. Lapinska, *BioMed Res. Int.*, **2016**, 1048320 (2016); https://doi.org/10.1155/2016/1048320
9. R. Fopase, S.R. Pathode, S. Sharma, P. Datta and L.M. Pandey, *Polym.-Plast. Technol. Mater.*, **59**, 2076 (2020); https://doi.org/10.1080/25740881.2020.1784222
10. D. Bourgeois, C. Inquimbert, L. Ottolenghi and F. Carrouel, *Microorganisms*, **7**, 424 (2019); https://doi.org/10.3390/microorganisms7100424
11. J. Jiang, J. Pi and J. Cai, *Bioinorg. Chem. Appl.*, **2018**, 1062562 (2018); https://doi.org/10.1155/2018/1062562
12. S.E. Jin, J.E. Jin, W. Hwang and S.W. Hong, *Int. J. Nanomedicine*, **14**, 1737 (2019); https://doi.org/10.2147/IJN.S192277
13. M. Bandeira, M. Giovanela, M. Roesch-Ely, D.M. Devine and J. da Silva Crespo, *Sustain. Chem. Pharm.*, **15**, 100223 (2020); https://doi.org/10.1016/j.scp.2020.100223
14. G.S. Thirumoorthy, O. Balasubramaniam, P. Kumaresan, P. Muthusamy and K. Subramani, *Bionanoscience*, **11**, 172 (2021); https://doi.org/10.1007/s12668-020-00817-y
15. M.D. Jayappa, C.K. Ramaiah, M.A.P. Kumar, D. Suresh, A. Prabhu, R.P. Devasya and S. Sheikh, *Appl. Nanosci.*, **10**, 3057 (2020); https://doi.org/10.1007/s13204-020-01382-2
16. S.M. Pituru, M. Greabu, A. Totan, M. Imre, M. Pantea, T. Spinu, A.M.C. Tancu, N.O. Popoviciu, I.-I. Stanescu and E. Ionescu, *Materials*, **13**, 2894 (2020); https://doi.org/10.3390/ma13132894
17. R. Vivek, *J. Dent. Oral Health*, **3**, 1 (2017).
18. M. Cierech, J. Wojnarowicz, A. Kolenda, A. Krawczyk-Balska, E. Prochwicz, B. Wozniak, W. Lojkowski and E. Mierzwińska-Nastalska, *Nanomaterials*, **9**, 1318 (2019); https://doi.org/10.3390/nano9091318
19. S. Fu, Z. Sun, P. Huang, Y. Li and N. Hu, *Nano Mater. Sci.*, **1**, 2 (2019); https://doi.org/10.1016/j.nanoms.2019.02.006
20. S. Soltanian, M. Sheikhbahaei, N. Mohamadi, A. Pabarja, M.F.S. Abadi and M.H.M. Tahroudi, *Bionanoscience*, **11**, 245 (2021); https://doi.org/10.1007/s12668-020-00816-z
21. M.M. Khan, N.H. Saadah, M.E. Khan, M.H. Harunsani, A.L. Tan and M.H. Cho, *Mater. Sci. Semicond. Process.*, **91**, 194 (2019); https://doi.org/10.1016/j.mssp.2018.11.030
22. J. Santhoshkumar, S.V. Kumar and S. Rajeshkumar, *Resource-Effic. Technol.*, **3**, 459 (2017); https://doi.org/10.1016/j.reffit.2017.05.001
23. S. Vijayakumar, Z.I. González-Sánchez, B. Malaikozhundan, K. Saravanakumar, M. Divya, B. Vaseeharan, E.F. Durán-Lara and M.-H. Wang, *J. Cluster Sci.*, **32**, 1129 (2021); https://doi.org/10.1007/s10876-020-01870-z
24. G.A. O'Toole, *J. Vis. Exp.*, **47**, e2437 (2011).
25. G. Prasannaraj and P. Venkatachalam, *J. Cluster Sci.*, **28**, 645 (2017); https://doi.org/10.1007/s10876-017-1160-x

26. M. Cierech, A. Kolenda, A.M. Grudniak, J. Wojnarowicz, B. Wozniak, M. Golac, E. Swoboda-Kopec, W. Lojkowski and E. Mierzwińska-Nastalska, *Int. J. Pharm.*, **510**, 323 (2016); https://doi.org/10.1016/j.ijpharm.2016.06.052
27. G. Carpenter, *Clin. Dent. Rev.*, **2**, 24 (2018); https://doi.org/10.1007/s41894-018-0033-5
28. N. Najim, R. Rusdi, A.S. Hamzah, Z. Shaameri, M.M. Zain and N. Kamarulzaman, *J. Nanomater.*, **2014**, 694737 (2014); https://doi.org/10.1155/2014/694737
29. S. Vijayakumar, B. Vaseeharan, R. Sudhakaran, J. Jeyakandan, P. Ramasamy, A. Sonawane, A. Padhi, P. Velusamy, P. Anbu and C. Faggio, *J. Cluster Sci.*, **30**, 1465 (2019); https://doi.org/10.1007/s10876-019-01590-z
30. A.M. Awwad, M.W. Amer, N.M. Salem and A.O. Abdeen, *Chem. Int.*, **6**, 151 (2020).
31. S.K. Bajpai, M. Jadaun and S. Tiwari, *Carbohydr. Polym.*, **153**, 60 (2016); https://doi.org/10.1016/j.carbpol.2016.07.019
32. D. Jain, A.A. Shivani, H. Bhojiya, H. Singh, H.K. Daima, M. Singh, S.R. Mohanty, B.J. Stephen and A. Singh, *Front. Chem.*, **8**, 778 (2020); https://doi.org/10.3389/fchem.2020.00778
33. Z. Song, T.A. Kelf, W.H. Sanchez, M.S. Roberts, J. Ricka, M. Frenz and A.V. Zvyagin, *Biomed. Opt. Express*, **2**, 3321 (2011); https://doi.org/10.1364/BOE.2.003321
34. W. Muhammad, N. Ullah, M. Haroon and B.H. Abbasi, *RSC Adv.*, **9**, 29541 (2019); https://doi.org/10.1039/C9RA04424H
35. A. Aldalbahi, S. Alterary, R. Ali Abdullrahman Almoghim, M.A. Awad, N.S. Aldosari, S. Fahad Alghannam, A. Nasser Alabdan, S. Alharbi, B. Ali Mohammed Alateeq, A. Abdulrahman Al Mohsen, M.A. Alkathiri and R. Abdulrahman Alrashed, *Molecules*, **25**, 4198 (2020); https://doi.org/10.3390/molecules25184198
36. M.M. Chikkanna, S.E. Neelagund and K.K. Rajashekarappa, *SN Appl. Sci.*, **1**, 117 (2018); https://doi.org/10.1007/s42452-018-0095-7
37. R. Rekha, S. Mahboob, A.K. Ramya, S. Kerthekeyan, M. Govindarajan, K.A. Al-Ghanim, F. Al-Misned, Z. Ahmed and B. Vaseeharan, *J. Cluster Sci.*, **32**, 843 (2021); https://doi.org/10.1007/s10876-020-01849-w
38. K.R. Raghupathi, R.T. Koodali and A.C. Manna, *Langmuir*, **27**, 4020 (2011); https://doi.org/10.1021/la104825u
39. E.J. Ibrahem, K.M. Thalij, M.K. Saleh and A.S. Badawy, *Am. J. Biochem. Biotechnol.*, **13**, 63 (2017); https://doi.org/10.3844/ajbbsp.2017.63.69
40. S.V. Gudkov, D.E. Burmistrov, D.A. Serov, M.B. Rebezov, A.A. Semenova and A.B. Lisitsyn, *Front. Phys.*, **9**, 641481 (2021); https://doi.org/10.3389/fphy.2021.641481
41. N. Padmavathy and R. Vijayaraghavan, *Sci. Technol. Adv. Mater.*, **9**, 035004 (2008); https://doi.org/10.1088/1468-6996/9/3/035004
42. S. Kulshrestha, S. Khan, R. Meena, B.R. Singh and A.U. Khan, *Biofouling*, **30**, 1281 (2014); https://doi.org/10.1080/08927014.2014.983093
43. S. Vijayakumar and B. Vaseeharan, *Adv. Powder Technol.*, **29**, 2331 (2018); https://doi.org/10.1016/j.apt.2018.06.013
44. S.G. Ali, M.A. Ansari, M.A. Alzohairy, M.N. Alomary, M. Jalal, S. Al-Yahya, S.M.M. Asiri and H.M. Khan, *Antibiotics*, **9**, 260 (2020); https://doi.org/10.3390/antibiotics9050260
45. R. Pati, R.K. Mehta, S. Mohanty, A. Padhi, M. Sengupta, B. Vaseeharan, C. Goswami and A. Sonawane, *Nanomedicine*, **10**, 1195 (2014); https://doi.org/10.1016/j.nano.2014.02.012
46. M.H. Sangani, M.N. Moghaddam and M. Forghanifard, *Nanomed. J.*, **2**, 121 (2015).
47. M. Saadat, S. Roudbar Mohammadi, M. Yadegari, M. Eskandari and R. Khavari-nejad, *J. Jahrom Univ. Med. Sci.*, **10**, 13 (2012) .
48. S. Nemati, H.A. Hosseini, A. Hashemzadeh, M. Mohajeri, Z. Sabouri, M. Darroudi and R. Kazemi Oskuee, *Mater. Res. Express*, **6**, 125016 (2019); https://doi.org/10.1088/2053-1591/ab46fb
49. Z. Sanaeimehr, I. Javadi and F. Namvar, *Cancer Nanotechnol.*, **9**, 3 (2018); https://doi.org/10.1186/s12645-018-0037-5
50. M. Dhamodaran and S. Kavitha, *Int. J. Pharm. Sci. Nanotechnol.*, **8**, 3018 (2015).